ISBN: 978-3-95450-208-0 doi:10.18429/JACoW-IPAC2019-THPGW045

A SIMPLE WAY TO INTRODUCE AN AJUSTABLE FEMTOSECOND PRE-PULSE TO ENHANCE LASER-DRIVEN PROTON ACCELERATION*

P Wang, Y Shou, Z Pan, S Xu, D Wang, J Liu, Z Cao, Z Mei, D Kong, Y Geng, Y Zhao, H Lu, C Lin, X Yan, W Ma† Institute of Heavy Ion Physics, Peking University, Beijing, 100871, China
Y Gao, Fakultät für Physik, Ludwig-Maximilians-Universität München,D-85748, Garching, Germany

Abstract

We demonstrate a simple way to introduce a femtosecond pre-pulse with adjustable intensity and delay without using an additional compressor to enhance laser-driven proton acceleration. Targets with different thicknesses were shoot at normal incidence by varying the pre-pulses. Experimental results show that significant enhancement of the proton energy can be achieved when the intensity of pre-pulse is optimized. Density profile of preplasma was obtained by hydrodynamic simulations. PIC simulations reveal that the preplasma generated by a femtosecond pre-pulse can increase the intensity of main pulse.

INTRODUCTION

Laser-driven ion acceleration has been an attractive field over the past decades. Its accelerating gradient is of TV/m, three orders compared to that of conventional accelerators. Proton beams accelerated in the interaction of ultra-short pulse and plasma show some unique advantages: short duration, small source size [1] and small emittance [2, 3], which benefit wide potential applications and basic science, such as radiotherapy [4], radiography [5] and tools for investigating nuclear [6] and astrophysical questions [7].

Great efforts have been made to increase the cut-off energy theoretically and experimentally, including target ablation [8, 9], double-layer target [10, 11] and hybrid acceleration scheme [12]. It has been demonstrated the preplasma generated in the target ablation process can increase the laser absorption and improve the quality of laser when parameters are appropriate. McKenna *et al.* [9] demonstrated preplasma with an 30-60 μm underdense scale length at the front side of targets can enhance proton acceleration. Amplified spontaneous emission (ASE) [13, 14] at the leading edge of the main pulse and pre-pulses (intrinsic [15] or external [9, 16]) are main methods to produce preplasma. Kaluza *et al.* [13] found the optimal thickness of targets for maximum proton energy strongly depends on the duraion of pre-pulse. Recently, more attention was attracted on using femtosecond pre-pulse to enhance proton acceleration. Zhou *et al.* [17] developed a numerical model describing the evolution of targets as a function of intensity and interval time for fs pre-pulse. Yogo *et al.* [15] found the intrinsic femtosecond pre-pulse, which comes from the leakage of a regenerative amplifier at 9 ns before main pulse, can increase proton energy. Glinec *et al.* [18] utilized an additional femtosecond beam from a second compressor as pre-pulse to generate the preplasma. As for the intrinsic femtosecond pre-pulses, it's difficult to adjust the intensity of pre-pulse and delay. In the two-beam scheme, achieving right timing and good overlap of the focuses requires quite a lot efforts.

In this paper, we report on experimental results using an adjustable-femtosecond pre-pulse to enhance proton acceleration in a simple way. The pre-pulse and main pulse were sent to the targets in sequence through the same beamline. Preliminary parametric study about the thickness of targets and intensity of pre-pulse shows that preplasma at the front of thick targets can make a contribution to proton acceleration. Hydrodynamic and PIC simulations reveal that relativistic self-focusing happens in the preplasma increasing the intensity of main pulse.

EXPERIMENTAL SETUP

The experiments were performed using the Compact LAser Plasma Accelerator (CLAPA) system at Peking University based on Ti: Sapphire with double CPA systems.

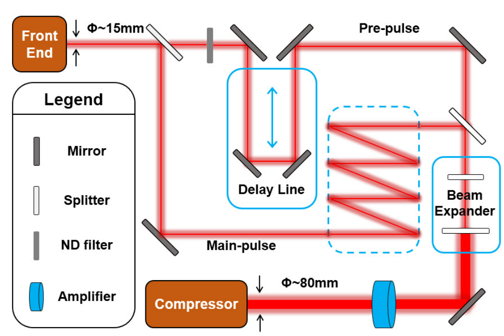

Figure 1: Experimental Setup.

The central wavelength is at 800 nm and its bandwidth is 45 nm. A cross-polarized wave (XPW) filter [19] is installed between the regenerative amplifier and the PW stretcher to enhance the laser temporal contrast. Nanosecond contrast (10^{-10}) is measured by InGaAs detector with a high speed oscilloscope, and the results [20] using a third order scanning autocorrelator show that the laser contrast is 10^{-10} @ 40 ps, 10^{-9} @ 38 ps and 19 ps. The *p*-polarized laser pulse is focused onto targets by an f/3.75 off-axis parabolic (OAP) mirror with an energy of 1.3 J and a duration of 33 fs. The diameter of focal spot (FWHM) is 6 um, with 32% of energy in it, giving a peak intensity of $4.5 \times 10^{19}\mathrm{W/cm^2}$. Concerning to the laser contrast measured above, maximum intensity

* Work supported by National Natural Science Foundation of China (Grants No. 11535001, 11575011, 11775010, 61631001, 8200903880, 8201200509).
† wenjun.ma@pku.edu.cn

ISBN: 978-3-95450-208-0 doi:10.18429/JACoW-IPAC2019-THPGW045

of the intrinsic pre-pulse is around 10^{10}W/cm^2. The experimental setup is shown in Fig. 1. The diameter of spot at the output of front end was 15 mm with a duration of 200 ps. Two splitters were used to separate the main pulse and combine pulses together. Pre-pulse was delayed by the delay line and attenuated by neutral density filters. Only small and thin mirrors and filters were needed introducing few group delay dispersion (GDD) before the beam expander. The duration of the deliberate pre-pulse was therefore assumed same as that of main pulse, leading to an intensity up to 10^{17}W/cm^2. The interval time can be controlled by a linear translation stage varying from 0 to 4 ns.

The targets were plastic targets made of polyvinyl formal with thicknesses varying from 50 nm to 2 um. Protons were detected by a thomson parabola spectrometer (TPS) placed in the normal direction of target. The acceptance angle was 2.72×10^{-7}sr with a 200 μm -diameter collimated pinhole. A microchannel plate (MCP) coupled with a phosphor screen was used to record the ion traces, followed by an Electron Multiplying Charge Coupled Device camera (EMCCD).

RESULTS

Preliminary parametric study is focused on the thickness of targets and varying intensities of pre-pulse with a fixed interval time (1.7 ns). Fig. 2 shows a pre-pulse with intensity of 4.4×10^{14}W/cm^2 results in a decrease of proton energy for thin targets (tens to hundreds of nanometers) and a significant enhancement can present for 2 micrometers tar-

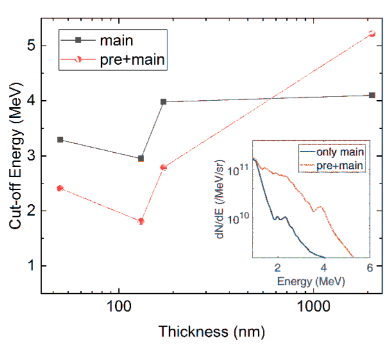

Figure 2: Experimental measurements of proton energy as a function of target thickness with or without the deliberate pre-pulse for fixed $I_{prepulse} = 4.4\times10^{14}$W/cm^2. The inset is an typical proton energy spectrum measured by TPS.

gets. Corresponding proton energy spectrum showed in the inset illustrates the increase in energy and charge. MULTI-IFE [21] 1D is used to simulate the electron density profile before main pulse interacting with target, as shown in Fig. 3. For wavelength of 800 nm used in our system, the critical density (N_c) is about 1.72×10^{21}/cm^3. The density of thin targets drops lower than N_c, which is transparent to the main pulse. For thicker (2 um) targets, there still exists a relatively sharp edge at the rear side of target able to sustain a strong sheath field.

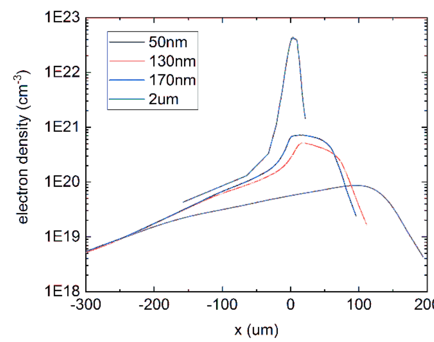

Figure 3: The electron density profile simulated by the MULTI-IFE code for 50 nm, 130 nm, 170 nm, 2 um target respectively.

Using 2-micrometer targets the effects of varying intensity of pre-pulse were studied and Fig. 4 shows the results. We can infer that plasma expansion at the rear target can reduce the sheath field when intensity of pre-pulse is too strong from the MULTI-IFE simulation results. Pre-pulse with appropriate intensity can produce preplasma at the front side of targets, which is beneficial to proton acceleration. Results from a 2D PIC simulation (Fig. 5) show that relatively nonlinear effects occur in preplasma including relativistic self-focusing and pulse front steepening. This shorten the duration of main pulse in time domain and spot size in the focal spot, which can increase the intensity of main pulse. Meanwhile, electrons accelerated by direct laser acceleration (DLA) can enhance the sheath field.

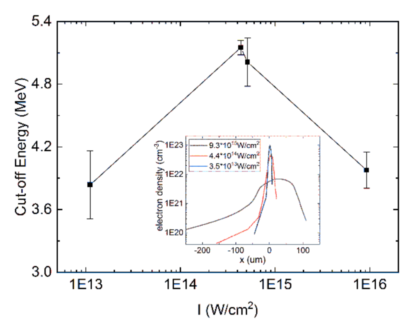

Figure 4: The cut-off proton energy for different pre-pulse intensity using 2-micrometer targets. The inset shows the corresponding simulation results using MULTI-IFE code.

CONCLUSION

By introducing a splitting beam at the front end of a typical Ti: Sapphire laser system, we generate a femtosecond pre-pulse with adjustable intensity and delay without using an additional compressor. Preliminary results about the effects of femtosecond pre-pulse on proton acceleration proves that a pre-pulse with appropriate intensity matching the targets can increase proton energy.

ISBN: 978-3-95450-208-0 doi:10.18429/JACoW-IPAC2019-THPGW045

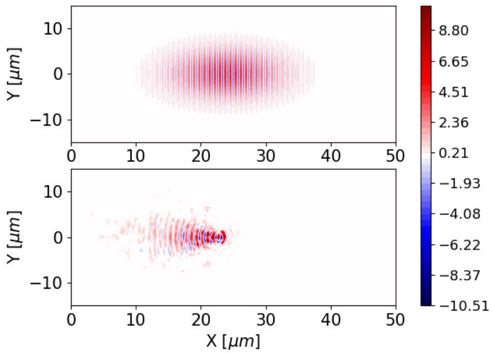

Figure 5: The normalized laser electric field Ey at 50 T. The upper shows the electric field profile without fs pre-pulse, and the lower shows the results with fs pre-pulse.

METHODS

Hydrodynamic Simulations Hydrodynamic code Multi-IFE is employed to obtain the distribution of electron density of targets irradiated by the fs pre-pulse. The pre-pulse has the duration of 33 fs, with intensity ranging from $3.5 \times 10^{13}\mathrm{W/cm^2} - 9.27 \times 10^{15}\mathrm{W/cm^2}$, and wavelength $\lambda = 800$nm. The thickness of targets includes 50 nm, 130 nm, 170 nm and 2000 nm, and their initial density ρ_0 is $1.20\mathrm{g/cm^3}$.

PIC Simulations PIC simulations were performed for the 2 μm target in the condition of fs pre-pulse and without it. The 2D EPOCH code was simulated on the high performance computing platform of Peking University. We set the boundary of the box $80\mu m \times 30\mu m$ and divided it into 8000×600 cells with each filled with 20 macro particles. All the boundary conditions were set as free space. The wavelength of laser is 800 nm and the profile of linearly-polarized laser is set as $\mathrm{a} = \mathrm{a_0 exp}(-\frac{(\mathrm{x}-\mathrm{x_0})^2}{\mathrm{w_0^2}})\mathrm{exp}(-\frac{(\mathrm{t}-\mathrm{t_0})^2}{\tau^2})$, where the values of a_0, x_0, w_0, t_0 and τ are 4.56, 40 μm, $6\mu m$, 20 T and 10 T, respectively (the peak intensity of laser is $4.45 \times 10^{19}\mathrm{W/cm^2}$). We use the output of MULTI-IFE simulations as the initial electron density distribution in the case of fs pre-pulse. The targets are set fully ionized in both cases and the ratio of hydrogen, carbon and oxygen is 8:5:2.

REFERENCES

[1] Nürnberg, F. *et al.,* "Radiochromic Film Imaging Spectroscopy of Laser-accelerated Proton Beams," Review of scientific instruments 80.3 (2009): 033301.

[2] Borghesi, M. *et al.,* "Multi-MeV Proton Source Investigations in Ultraintense Laser-foil Interactions," Physical Review Letters 92.5 (2004): 055003.

[3] Cowan, T. E. *et al.,* "Ultralow Emittance, Multi-MeV Proton Beams from a Laser Virtual-cathode Plasma Accelerator," Physical review letters 92.20 (2004): 204801.

[4] Kraft, S. D. *et al.,* "Dose-dependent biological damage of tumour cells by laser-accelerated proton beams." New Journal of Physics 12.8 (2010): 085003.

[5] Borghesi, M. *et al.,* "Proton imaging detection of transient electromagnetic fields in laser-plasma interactions." Review of Scientific Instruments 74.3 (2003): 1688-1693.

[6] Roth, M. *et al.,* "Fast ignition by intense laser-accelerated proton beams." Physical Review Letters 86.3 (2001): 436.

[7] Pelka, A. *et al.,* "Ultrafast melting of carbon induced by intense proton beams." Physical review letters 105.26 (2010): 265701.

[8] Zhao, S. *et al.,* "Ion acceleration enhanced by target ablation." Physics of Plasmas 22.7 (2015): 073106.

[9] McKenna, P. *et al.,* "Effects of front surface plasma expansion on proton acceleration in ultraintense laser irradiation of foil targets." Laser and Particle Beams 26.4 (2008): 591-596.

[10] Bin, J. H. *et al.,* "Ion acceleration using relativistic pulse shaping in near-critical-density plasmas." Physical review letters 115.6 (2015): 064801.

[11] Ma, W. J. *et al.,* "Laser acceleration of highly energetic carbon ions using a double-layer target composed of slightly underdense plasma and ultrathin foil." Physical Review Letters 122.1 (2019): 014803.

[12] Higginson, A. *et al.,* "Near-100 MeV protons via a laser-driven transparency-enhanced hybrid acceleration scheme." Nature communications 9.1 (2018): 724.

[13] Kaluza, Malte *et al.,* "Influence of the laser prepulse on proton acceleration in thin-foil experiments." Physical review letters 93.4 (2004): 045003.

[14] Wang, D. H. *et al.,* "Enhanced proton acceleration from an ultrathin target irradiated by laser pulses with plateau ASE." Scientific reports 8.1 (2018): 2536.

[15] Yogo, Akifumi. *et al.,* "Laser prepulse dependency of proton-energy distributions in ultraintense laser-foil interactions with an online time-of-flight technique." Physics of plasmas 14.4 (2007): 043104.

[16] Maksimchuk, Anatoly. *et al.,* "Forward ion acceleration in thin films driven by a high-intensity laser." Physical Review Letters 84.18 (2000): 4108.

[17] Zhou, M. L. *et al.,* "The impact of femtosecond pre-pulses on nanometer thin foils for laser-ion acceleration." Plasma Physics and Controlled Fusion 59.5 (2017): 055020.

[18] Glinec, Yannick. *et al.,* "Evolution of energy spectrum from laser-accelerated protons with a 100 fs intense prepulse." Applied Physics B 93.2-3 (2008): 317-321.

[19] Geng, Y. X. *et al.,* "Influences of quadratic spectral phase on characteristics of two crystal cross-polarized generation with femtosecond pulses." Acta Physica Sinica, 2017, 66(4): 040601.

[20] Shou, Y. R. *et al.,* "Laser proton accelerator with improved repeatability at Peking University." Journal of Physics: Conference Series. Vol. 874. No. 1. IOP Publishing, 2017.

[21] Ramis, R. *et al.,* "MULTI-IFE—A one-dimensional computer code for Inertial Fusion Energy (IFE) target simulations." Computer Physics Communications 203 (2016): 226-237.